Joule

CellPress

Perspective

# Greening Ammonia toward the Solar Ammonia Refinery

Lu Wang,[1] Meikun Xia,[1] Hong Wang,[2] Kefeng Huang,[3] Chenxi Qian,[1] Christos T. Maravelias,[3] and Geoffrey A. Ozin[1,*]

**In light of the targets set out by the Paris Climate Agreement and the global energy sector's ongoing transition from fossil fuels to renewables, the chemical industry is searching for innovative ways of reducing greenhouse gas emissions associated with the production of ammonia. To address this need, research and development is under way around the world to replace the century-old Haber-Bosch process for manufacturing ammonia from $N_2$ and $H_2$, powered by renewable electricity. This involves replacing $H_2$ obtained from steam-reformed $CH_4$ to $H_2$ that is instead obtained from electrolyzed $H_2O$. This transition will enable the changeover from the Haber-Bosch production of $NH_3$ to electrochemical, plasma chemical, thermochemical, and photochemical generation of $NH_3$. If ammonia can eventually be produced directly from $N_2$ and $H_2O$ powered by just sunlight, at a technologically significant scale, efficiency, and cost, in a "solar ammonia refinery," green ammonia can change the world!**

## Ammonia Background

Fritz Haber, a German chemist, Nobel Laureate in chemistry 1918, invented a way to make the nitrogen in air available to plants by converting it, together with hydrogen, into ammonia. Working with Carl Bosch at BASF in Ludwigshafen, Germany, he developed the heterogeneous catalytic Haber-Bosch process,[1–5] which first operated on an industrial scale for the production of ammonia in 1913. For developing this process, Carl Bosch received the Nobel Prize in Chemistry 1931. Surprisingly, the best catalyst for the production of ammonia, discovered by Alwin Mittasch, was found to have a composition similar to "Gallivare" magnetite, a multi-component iron ore from northern Sweden with a composition composed of $Fe_3O_4$, CaO, $Al_2O_3$, MgO, and $Cr_2O_3$ component metal oxides.

This century-old process continues to produce more than 90% of ammonia today, used mainly as the precursor to nitrogen fertilizers, enabling farmers to provide a growing world population with a secure and affordable source of food.[6–8] Its use is so ubiquitous that nearly 80% of the nitrogen found in human tissues originates from the Haber-Bosch process.[9] Besides its use for the manufacture of fertilizer for agriculture, ammonia is also a hydrogen storage medium, chemical feedstock, clean burning fuel for transportation and the power generation sector, and refrigerant fluid.[10–13]

Ammonia is one of the largest-volume industrial chemicals synthesized in the world in terms of its energy use and carbon footprint. The global industrial complex makes around 500 Mt/year of nitrogen-containing fertilizer.[7,14] The current cost of ammonia is around US$500/t with a world value of about $250 billion.[15] Conservative estimates report 30%–50% of crop yields emanating from the use of natural or synthetic fertilizer.[16,17]

## Context & Scale

It is well known that the century-old Haber-Bosch process, $N_2 + 3H_2 \rightarrow 2NH_3$, is thermally powered by fossil energy, resulting in a greenhouse gas intensive process, which needs to be replaced by one driven instead by renewable energy. To address this issue, we need to replace the energy-intensive synthesis process of ammonia from $N_2$ and $H_2$ by one powered instead by renewable electricity. This involves replacing $H_2$ obtained from steam-reformed $CH_4$ to $H_2$ that is instead obtained from electrolyzed $H_2O$. Consequently, the required energy is dramatically decreased, and the conversion no longer requires $CH_4$ derived from natural gas because the $H_2$ comes directly from $H_2O$.

Herein, we present a critical overview of past and current research on ammonia synthesis that is envisioned to evolve to the "solar ammonia refinery" of the future. A high-level analysis of the energy requirements of the proposed greening ammonia strategies further supports the "solar ammonia refinery."

In the context of climate change, it is significant to note that the amount of $CO_2$ equivalents released into the atmosphere from the production of ammonia is around 400 Mt/year with 12 Gt/year of $CO_2$ equivalents produced from the entire ammonia food chain. This carbon footprint represents around 1.5% of all greenhouse gas emissions.[18] Of significance, to operate the Haber-Bosch process around 3%–5% of the world's natural gas production is consumed, which corresponds to about 1%–2% of the world's annual energy supply.[19–23]

The Haber-Bosch process, normally powered by fossil fuel, operates at extremely high temperatures (400°C–500°C) and pressures (100–200 atm), most commonly using an iron-based catalyst.[24–26] The Haber-Bosch process is energetically demanding and kinetically complex. Mechanistically it involves the dissociative adsorption of $N_2$ and reduction of surface nitride by $H_2$ passing through surface $NH_x$ intermediates, culminating with the formation and desorption of $NH_3$.[26,27] The overall conversion of $N_2$ and $H_2$ to $NH_3$ is 97%.[28] The Nobel Prize in Chemistry 2007 recognized the work of Gerhard Ertl, especially his elucidation of the mechanism of the ammonia synthesis reaction.

The extreme conditions required to drive the exothermic $N_2 + 3H_2 \rightarrow 2NH_3$ reaction originates in the equilibrium thermodynamics, which are unfavorable above 200°C and conflict with the kinetic performance of the catalyst that requires temperatures around 400°C–500°C to attain sufficient activity. As a compromise between the thermodynamics and kinetics of the Haber-Bosch process, it is necessary to operate at extremely high pressures, 100–200 atm, employing multiple passes and cooling between stages to optimize conversion. Motivation for ongoing research is aimed at lowering the pressure of the Haber-Bosch process, mainly related to the 50% capital cost of compression required to produce ammonia.[29]

The complexity of the process, appreciated by inspection of the flow diagram in Figure 1, comprises the following steps:[30]

(i) catalytic steam reforming of $CH_4$ forms CO and $H_2$;
(ii) catalytic water gas shift makes more $H_2$ from the CO and converts the CO into $CO_2$;
(iii) removal of the $CO_2$ by absorption or adsorption media;
(iv) catalytic methane formation removes residual CO and $CO_2$ from the $H_2$;
(v) purification of $H_2$ and $N_2$;
(vi) catalytic Haber-Bosch process makes ammonia;
(vii) purification of ammonia by separation from unreacted $H_2$ and $N_2$ by refrigeration.

The composition of the product stream, which contains $NH_3$, $H_2$, and $N_2$, depends upon the equilibrium thermodynamics at the operating conditions of temperature and pressure, flow rate, and $N_2/H_2$ stoichiometric ratio. The reaction kinetics are determined by the choice of catalyst and reactor design.

## Ammonia Produced from Renewable Energy

With the above background on conventional $NH_3$ technology, one would think there has to be a greener and simpler way of making $NH_3$ with a lower carbon footprint than practiced in the fossil energy-intensive Haber-Bosch process (Figure 2).[26,31–33]

Of the 60 million tons of $H_2$ produced annually for industrial purposes, 95% comes from fossil gas, oil, and coal, and the rest from $H_2O$ electrolysis.

[1]Solar Fuels Group, Chemistry Department, University of Toronto, Toronto, ON M5S 3H6, Canada

[2]Key Laboratory of Functional Polymer Materials, Ministry of Education, Institute of Polymer Chemistry, Nankai University, Tianjin 300071, P.R. China

[3]Department of Chemical and Biological Engineering, University of Wisconsin–Madison, Madison, WI 53706, USA

*Correspondence: gozin@chem.utoronto.ca

https://doi.org/10.1016/j.joule.2018.04.017

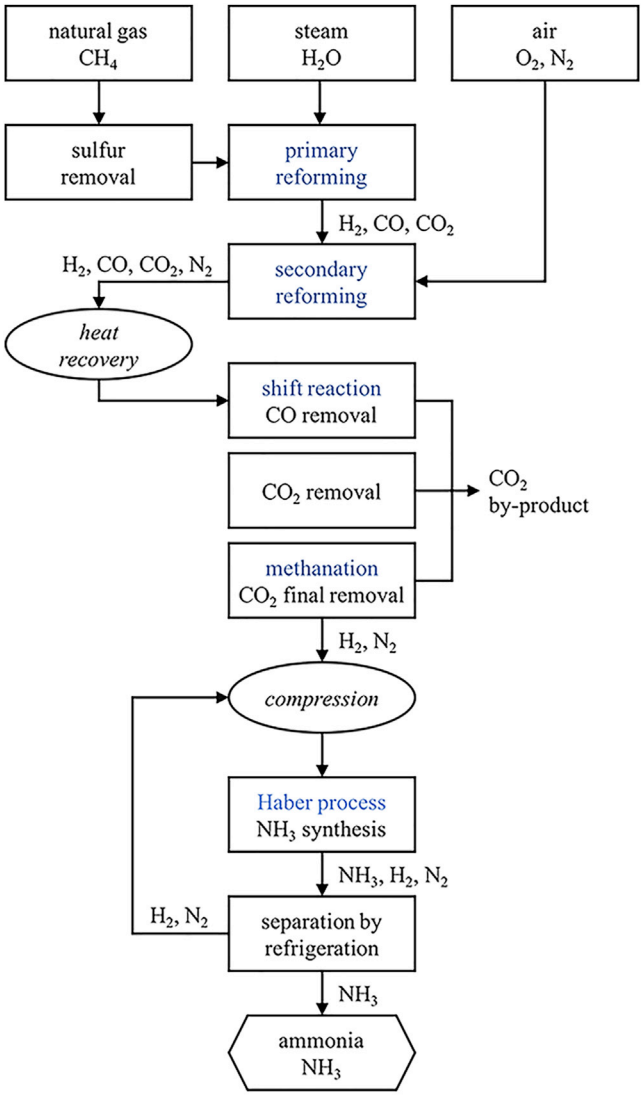


**Figure 1. Flow Diagram for the Multi-step Haber-Bosch Ammonia Production Process**
Graphic adapted from original source: University of York, 2013.

About half of the $H_2$ produced today feeds the Haber-Bosch process for making $NH_3$. In the quest for "green ammonia," it is noteworthy that because of recent cost reductions in renewable electricity, especially in geographic locations that are well endowed with solar and wind resources, the large-scale water electrolysis-based production of $NH_3$ can begin to compete with that dependent on steam reforming of natural gas. In these ideal locations, the cost of solar and wind electricity could be in the range of $30/MWh, which translates into $H_2$ from $H_2O$ electrolysis around $2/kg, a cost competitive with steam methane reforming.[34,35]

Indeed, the "green ammonia" challenge has inspired a flurry of activity in alternative methods for enabling the $N_2$ reduction reaction,[32,36–38] the main ones of which employ electrocatalysis,[10,21,39–46] bio-catalysis,[47,48] thermo-catalysis,[49–51] plasma-catalysis,[52,53] and photocatalysis,[54–58] powered by renewable energy, both solar and wind.

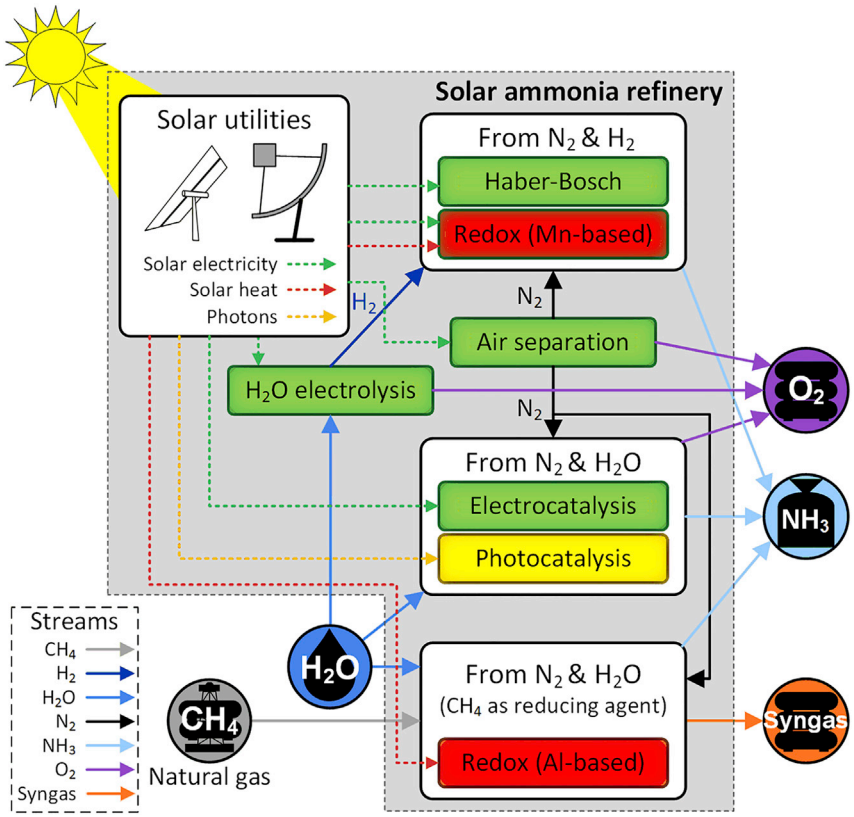


**Figure 2. The Solar Ammonia Refinery of the Future: Possible Pathways for Producing Ammonia from Renewable Energy**

Solar ammonia feedstocks ($N_2$, $H_2$/$H_2O$, and solar energy) are produced on-site and/or transported to the solar refinery. Solar energy provides solar utilities in the form of electricity, heating, and photons that are used in the solar refinery to convert $N_2$ and $H_2$/$H_2O$ into ammonia. The conversion can be categorized into three principal routes: (1) $NH_3$ synthesis from $N_2$ and $H_2$, (2) $NH_3$ synthesis from $N_2$ and $H_2O$ while co-producing $O_2$, and (3) $NH_3$ synthesis from $N_2$ and $H_2O$ using $CH_4$ as a reducing agent with co-production of syngas.

"All-electric" powered ammonia synthesis processes have been demonstrated in America, Australia, Africa, Canada, Germany, the Middle East, Norway, and the United Kingdom. It is impressive that a small-scale solar ammonia facility has been operating for a few years at Pinehurst Farm in Iowa (Schmuecker Pinehurst Farm LLC).[59] On this farm, solar-powered electrolysis and pressure swing systems generate, from well water and air, pure $H_2$ and $N_2$, which are compressed and fed into a Haber-Bosch ammonia generation facility. The ammonia thus produced fertilizes its cornfields and fuels its tractors.

Construction of a larger yet similarly conceived solar ammonia facility is underway near Pilbara, Western Australia (Yara).[60] Desalination of seawater by reverse osmosis yields pure $H_2O$. The $H_2O$ is the source of $H_2$ generated by electrolysis. Cryogenic air separation provides $N_2$ and $O_2$, whereby the $O_2$ has considerable commercial value in many applications, including rocket fuel, welding, antibacterial applications, and medicine. The renewable forms of $N_2$ and $H_2$ are the feedstock for the Haber-Bosch process. The goal is to evaluate the energy and economic flows of the process and determine the best pathways to commercialization, especially in countries that have large amounts of renewable electricity.

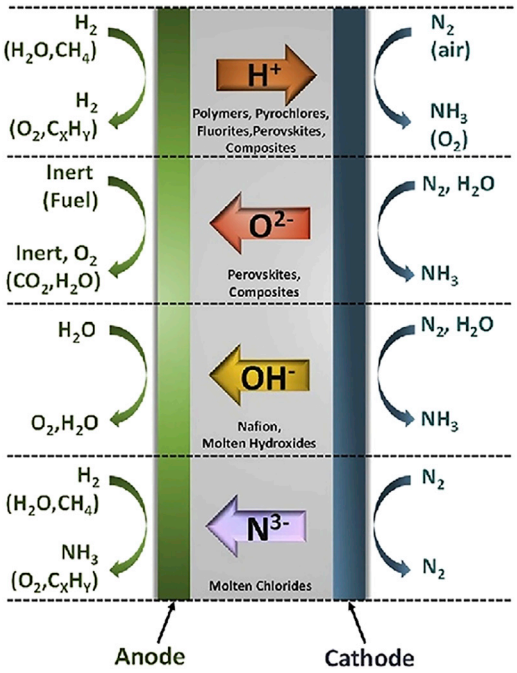


**Figure 3. Schematic Depicting the Four Main Strategies, Electrodes, and Electrolyte Designs for the Electrochemical Synthesis of $NH_3$ from $N_2$, $H_2$, and $H_2O$, and a Source of Electricity, Preferably Renewable**

Reproduced from Kyriakou et al.,[39] with permission. Copyright 2016, Elsevier B.V.

Another all-electric-based ammonia factory, Sable Chemical Industries Limited in Zimbabwe, Africa, has the world's largest electrolysis plant to provide the renewable $H_2$ for ammonia and ammonium nitrate synthesis.[61] The $N_2$ comes from air separation with subsequent purification and compression steps. A typical Haber-Bosch process can then produce the ammonia and ammonium nitrate obtained via sparging ammonia through nitric acid solution. This factory has been in operation for decades with an annual production of 240,000 tons of ammonium nitrate.

Recently, a "globally significant demonstrator project" was announced by the government of South Australia, and the renewable hydrogen power plant, which includes a renewable ammonia demonstration plant, is to be built in Port Lincoln, South Australia with construction beginning in 2019.[62] Similar to Yara, the $H_2$ comes from water electrolysis using renewable electricity, the $N_2$ is obtained from the air, and the ammonia is produced with the obtained renewable $H_2$ and $N_2$ via a Haber-Bosch process. The capacity of the ammonia plant is expected to be around 610 tons of liquid ammonia per day.

It is worth noting that the Haber-Bosch production of ammonia operates as a continuous recycle process whereby each pass through the reactor converts only about 15% of the $N_2$ and $H_2$ to $NH_3$, yet with continuous recycling 97% overall conversion is achieved. The intermittency of solar and wind is therefore not a big problem because the $H_2$ and $N_2$ feedstocks can be produced when electricity is being generated and stored for later use. Nevertheless, some electricity storage would be needed to power the process at night.

Beyond Haber-Bosch, there has been increasing research activity over the past 20 years into the science underpinning the techno-economic feasibility of synthesizing ammonia electrochemically (Figure 3),[39] in cells that employ either aqueous,[33,63] molten salt,[41–43,64,65] or solid electrolytes.[66–68] These studies essentially are divided into three main groups that depend on the temperature of operation: high

temperature (T > 500°C), intermediate temperature (500°C > T > 100°C), and low temperature (T < 100°C).

Early work in this genre emerged from a collaboration between researchers at the University of Ontario Institute of Technology and Hydrofuel. They explored electrochemical ammonia synthesis using $H_2$ generated photoelectrochemically.[69] In one example, $H_2$ and $N_2$ in a molten hydroxide electrolyte with a nanostructured $Fe_3O_4$ catalyst and high-surface-area and nickel mesh electrodes, $NH_3$ was generated at ambient pressure in the temperature range 200°C–255°C. The maximum Faradaic efficiency at 210°C was reported at 9.3% with a $NH_3$ formation rate of $6.53 \times 10^{-10}$ mol/s $cm^2$ at 2 mA/$cm^2$ current density.

It is worth noting also that Hydrofuel built the first car fueled by $NH_3$ in Canada.[70] Since that time, they have been developing diesel-$NH_3$ dual-fuel systems for various applications including heavy-duty vehicles, locomotives, ships, and stationary engines as well as commercialization of $NH_3$-based methods of chemically storing renewable energy.[71] It is noteworthy that replacing traditional fossil fuel with $NH_3$-based fuel is rather risky at the moment. As the exhaust gas from $NH_3$-based fuel could be nitrogen oxide ($NO_x$), which may raise further environmental issues. Thus, it is highly desirable to integrate a $NO_x$ purification technique into any ammonia energy-based system.

An extensive library of electroactive materials has been developed for ammonia synthesis, including metals Fe, Ni, Ru, Pd, Pt, and Au, alloys Ag-Pd and Ni-Cu,[72–74] simple and complex metal oxides,[68,75,76] metal nitrides,[5] carbon[54,77] and carbon nitrides,[78,79] and composites thereof.[20] For example, an electrochemical cell constructed with Ni electrodes and a ternary molten hydroxide (KOH/NaOH/CsOH) suspension of $Fe_2O_3$ nanoparticles produces $NH_3$ at a coulomb efficiency of 35% by electrolysis of air and steam at 200°C.[65]

Recently, *in situ* surface-enhanced infrared absorption spectroscopy has provided a detailed mechanistic description of the surface chemistry responsible for the electrochemical reduction of $N_2$ to $NH_3$, $N_2H_4$, and $H_2$ on a gold electrode in a 0.1 M KOH electrolyte (Figure 4A).[80] The detection of vibrational modes diagnostic of $NH_2$ bending at 1,453 $cm^{-1}$ and 1,298 $cm^{-1}$, together with N=N stretching at 1,109 $cm^{-1}$ served to identify surface reaction intermediates $N_2H_y$ ($1 < y < 4$). The observation of these fingerprint modes favors an associative reaction pathway, whereby adsorbed $N_2$ on Au is protonated and reduced to $N_2H_y$ ($1 < y < 4$) via a four-electron transfer process to $N_2H_4$ and/or a six-electron one to $NH_3$ (Figure 4B).

At the completion of this perspective, an exciting electrocatalyst was described that can enable nitrogen fixation. The electrocatalyst is composed of a nitrogen-doped nanoporous graphitic carbon membrane (NCM). It can electrochemically convert $N_2$ into $NH_3$ in an aqueous acidic solution at impressive rates and under ambient conditions for days (unpublished data, H.W., L.W., Q. Wang, S. Ye, W. Sun, Y. Shao, Z. Jiang, Q. Qiao, Y. Zhu, P. Song, et al.) (Figure 5). To elaborate, the faradaic efficiency and rate of production of $NH_3$ on the pristine form of the NCM electrode reached 5% and 0.08 g $m^{-2}$ $h^{-1}$, respectively. By functionalizing the NCM with Au nanoparticles, these performance metrics increased dramatically to ~20% and ~0.3 g $m^{-2}$ $h^{-1}$, respectively. These efficiencies and rates for the production of $NH_3$ at room temperature and atmospheric pressure are unprecedented.

Ultimately, the economics of any electrochemical ammonia process will be contingent on the cost of electricity, which will likely improve as renewable energy becomes

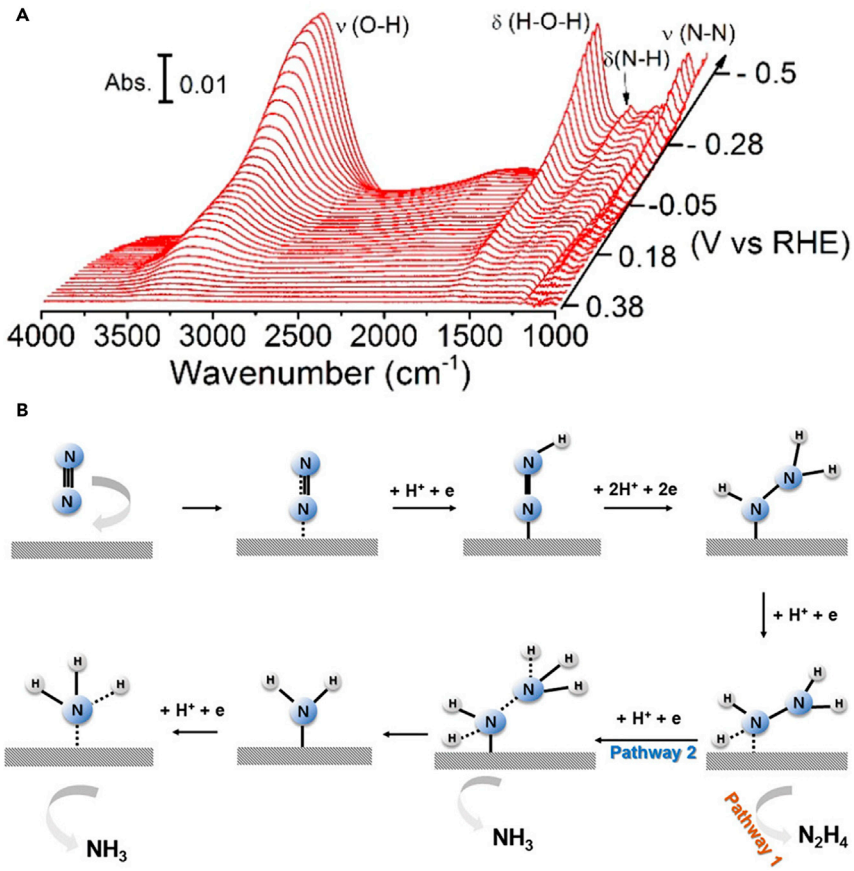


**Figure 4. Reaction Mechanisms of Nitrogen Reduction on Au Thin Film**

(A) Infrared spectra of the species observed on the surface of a gold electrode during the reduction of $N_2$ in a 0.1 M KOH electrolyte at different potentials.

(B) Proposed electrochemical $N_2$ reduction pathways on the surface of gold.

Reproduced from Yao et al.,[80] with permission. Copyright 2018, American Chemical Society.

increasingly available. Whatever the source of electricity, scaling the electrochemistry process to industrial proportions will require high faradaic efficiencies in excess of 50% and reaction rates of at least $10^{-7}$ mol $s^{-1}$ $cm^{-2}$.[39] At high temperatures, demonstrated faradaic efficiencies and rates are technologically viable but at low temperatures they are very small, typically below 1%.[81,82] A life-cycle analysis of competing electrochemical processes for $NH_3$ production ranked in decreasing order of efficiency the following technologies: solid oxide electrolytic cell, low-temperature solid-state ammonia synthesis (LT SSAS), Battolyser (battery-electrolyzer device), proton exchange membrane, and high-temperature SSAS (HT SSAS).[83] An all-electric "green ammonia" synthesis and energy-storage demonstrator, involving a collaborative venture between Siemens and Oxford and Cardiff Universities, is currently under evaluation at Appleton Rutherford Laboratories near Oxford, England.[84]

Key challenges confronting the creation of a viable electrochemical ammonia refinery include selective and stable catalysts and Faraday efficiencies that are on a par with the efficiency of the Haber-Bosch process.

A recent report demonstrates an innovative means of circumventing these hurdles.[85] It involves a novel electrochemical stepwise cycling strategy performed under

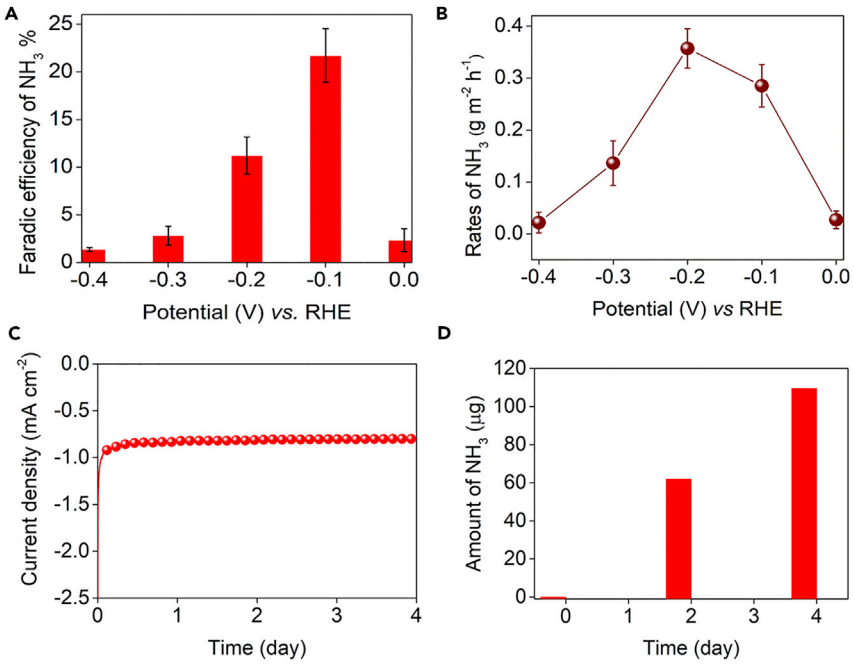


**Figure 5. Electrochemical Performance of the NCM-Au Nanoparticles in the Nitrogen Reduction Reaction**

(A) Faradaic efficiencies for $NH_3$ production versus applied potential at the NCM electrode (versus reversible hydrogen electrode [RHE]).

(B) The rates of $NH_3$ production on the NCM electrode at applied potentials (versus RHE).

(C) Chrono-amperometry results at the corresponding potentials (in A) with the highest faradaic efficiencies.

(D) The yields of $NH_3$ production at regular interval times on the NCM and NCM-Au NPs electrodes during a long-term operational stability test.

Error bars indicate the SD among three different tests.

ambient-pressure conditions. The cyclic process begins with molten lithium hydroxide (LiOH) electrolysis at 400°C–450°C to form Li metal, followed by nitridation of the Li to form lithium nitride ($Li_3N$) and completing the cycle with hydrolysis of the $Li_3N$ to produce $NH_3$ with regeneration of the LiOH. The process, illustrated in Figure 6, is powered by renewable electricity operated in a continuous stepwise cycle device, and can be run as a local production facility, suitable for the distributed production of $NH_3$. Because the $N_2$ reduction is separate from the protonation step, unlike aqueous electrochemical $NH_3$ synthesis methods the unwanted competing $H_2$ evolution reaction is avoided, thereby enabling unprecedented selectivity for $NH_3$ generation. At an operating cell potential near 4 V, the reported current efficiency of 88.5% is unprecedentedly high for the production of $NH_3$. A preliminary techno-economic analysis of the process, assuming the dominant cost is for the electricity driving the high-temperature LiOH electrolysis step, indicates it has the potential to function as a $NH_3$ synthesis complementary to the Haber-Bosch process.

Another strategy for synthesizing ammonia using renewable electricity exploits plasma chemistry.[52] To elaborate, an electrically excited plasma generates energized electrons, ions, atoms, radicals, molecules, and photons. Operating under ambient temperature and pressure conditions, the reactive species in a $H_2$-$N_2$ plasma provides an opportunity to synthesize $NH_3$ in a continuous process, powered by renewable electricity and under much milder conditions than those used in the high-temperature, high-pressure Haber-Bosch process. A recent example of plasma

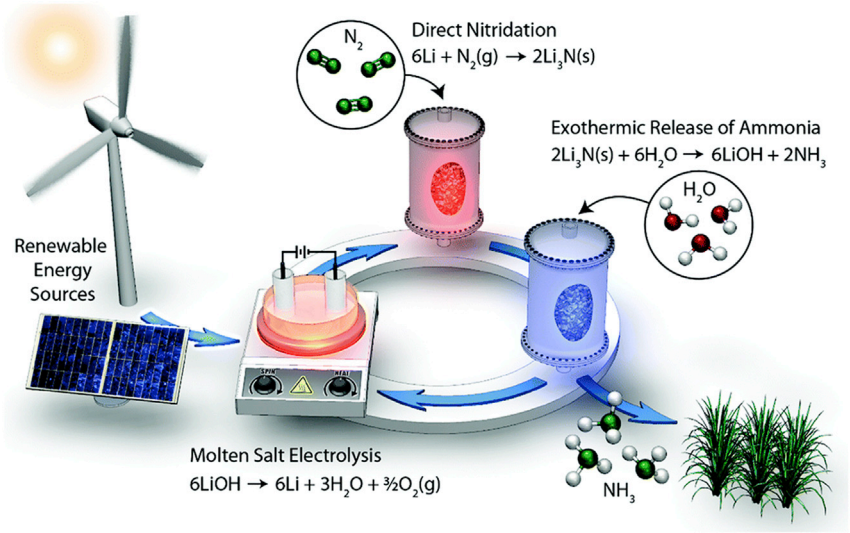


**Figure 6. Illustration of a Renewable Electricity-Powered Stepwise Lithium Cycling Process for the Sustainable Synthesis of $NH_3$ from $N_2$ and $H_2O$ under Ambient-Pressure Conditions**
Reproduced from McEnaney et al.,[85] with permission. Copyright 2017, Royal Society of Chemistry.

synthesis of ammonia employed a cesium-promoted ruthenium catalyst dispersed on a high-surface-area, mesoporous silica support.[86] By optimizing catalyst synthesis-structure-activity relations, controlling $N_2$-$H_2$ flow rates, minimizing $NH_3$ decomposition reactions, and adjusting voltage-frequency parameters of the plasma, it proved possible to achieve an ammonia synthesis efficiency of 1.7 g/kWh.

An alternative path for the production of $NH_3$ from $N_2$ and $H_2O$ makes use of concentrated solar energy to drive a thermochemical ammonia-producing redox cycle. In a recent example, the cycle begins with the reaction of a molybdenum or manganese nitride ($Mn_5N_2$, $Mo_2N$) and $H_2O$ at 400°C and 1 atm to produce $NH_3$ with concomitant formation of a metal oxide (MnO, $MoO_2$).[5] Subsequent reaction of the metal oxide with $N_2$ at 1,200°C and 1 atm reforms the metal nitride, thereby completing the solar thermal redox cycle (Figure 7).[5] For a large composition range of metal nitride-metal oxide redox couples found to be active for the solar thermal conversion of $N_2$ and $H_2O$ to $NH_3$, the energetically limiting reaction step is the production of oxygen vacancies in the metal oxide, which can react with $N_2$ to regenerate the metal nitride.

An energy-efficiency analysis of the molybdenum nitride ($Mo_2N$)-molybdenum oxide ($MoO_2$) solar thermal cyclic redox process for $NH_3$ operating at around 1,200°C, with solar thermal production of $H_2$, was in the range 23%–30%. A techno-economic evaluation of the process clarified its dependence on the high price of the solar thermal equipment ($90–$164/$m^2$), the yield of $NH_3$ (13.9%–100%), and the $NH_3$ sales price. The operation of a 900 t/day $NH_3$ solar thermal plant was shown to be economically viable with an acceptable $NH_3$ sales price of about $534 ± $28/t of $NH_3$.[58]

Because of the deficiency of thermochemical data for many of these materials, especially metal nitrides, density functional theory (DFT) calculations enable the prediction of their Gibbs formation energies up to the high operational temperatures of the solar thermal ammonia process. This can assist with the identification of optimal metal nitride-metal oxide redox pairs in the absence of experimental thermochemical data. In this way, it has proved possible to screen large libraries

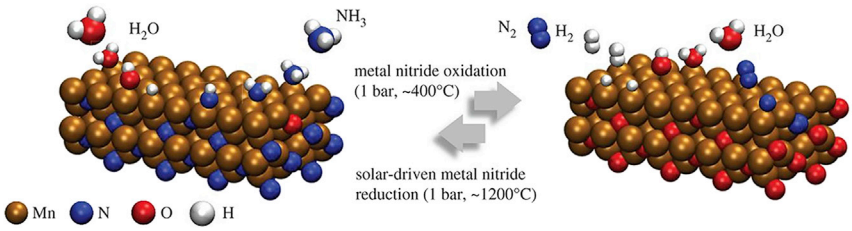


**Figure 7. Concentrated Solar Thermal, Atmospheric Pressure $NH_3$ Synthesis from $N_2$ and $H_2O$, Using a Metal Nitride-Metal Oxide Redox Cycle**

Reproduced from Michalsky et al.,[5] with permission. Copyright 2015, Royal Society of Chemistry.

of redox pairs, reaction schemes, and operating conditions to determine materials suitable for the solar thermal ammonia process. In this regard, a DFT computational materials study established perovskites as ideal candidates for metal oxide-metal nitride redox conversions.[38]

In ending this section, it is worth highlighting an innovative low-pressure strategy for synthesizing $NH_3$ from $H_2$ and $N_2$ in a novel kind of tubular metallic membrane reactor that separates the $N_2$ and $H_2$ dissociation-reaction zones. This strategy enhances the rate-determining adsorption-dissociation step of $N_2$ relative to $H_2$ and, hence, the rate of $NH_3$ formation. The construction of the reactor comprises a multilayer of a hydrogen permeable film made of Pd coated on a Cs-promoted Ru catalyst layer all supported on a porous ceramic tube. It is the combination of $H_2$ dissociation upon, and diffusion of H through, the hydrogen permeable layer, decoupled from the $N_2$ dissociation Cs-Ru catalyst surface, that allows low-pressure reaction of N and H and formation of $NH_3$, with reported rates of $6 \times 10^{-9}$ mol $cm^{-2}$ $s^{-1}$ at 500°C and 0.8 atm. The use of renewable energy to drive dissociation, diffusion, and reaction of $H_2$ and $N_2$ in the tubular metallic membrane reactor could enable the development of an ambient-pressure ammonia synthesis process that rivals emerging electrochemical ammonia technologies.[29]

## Advances in the Synthesis of Solar Ammonia from $N_2$ and $H_2O$ without the Use of Renewable Electricity or Heat

In the remainder of this article, highlighted are some emerging strategies for the production of solar ammonia, which exemplify methods that avoid the use of renewable electricity or heat but instead utilize only light.

The origin of this "all-solar" ammonia endeavor is traceable to early work in the field of semiconductor photocatalysis, where wide-bandgap nanostructured $TiO_2$ and $WO_3$ could produce $NH_3$ from $N_2$ and $H_2O$ in gaseous and aqueous phases.[87,88] The formation of $NH_3$ on these heterogeneous photocatalysts involves a reaction pathway whereby $H_2$ formed by the light-induced splitting of $H_2O$ reacts with $N_2$. A number of studies of non-stoichiometric oxygen-deficient metal oxide photocatalysts of the above type have invoked reduced oxidation state metal ions ($Ti^{3+}$, $W^{5+}$) and oxygen vacancies as the active sites for $N_2$ adsorption and reduction. Similarly, oxygen-deficient BiOBr nanosheets show formation of $NH_3$ from $N_2$, $H_2O$, and sunlight. By incorporating metal and metal oxide co-catalysts with these semiconductor nanomaterials, it is possible to enhance the yield of $NH_3$.

Five exciting recent advances in the emerging field of solar ammonia, namely the reduction of $N_2$ with $H_2O$ using sunlight under ambient conditions, exploit the unique chemical and physical properties of (i) biomimetic iron molybdenum

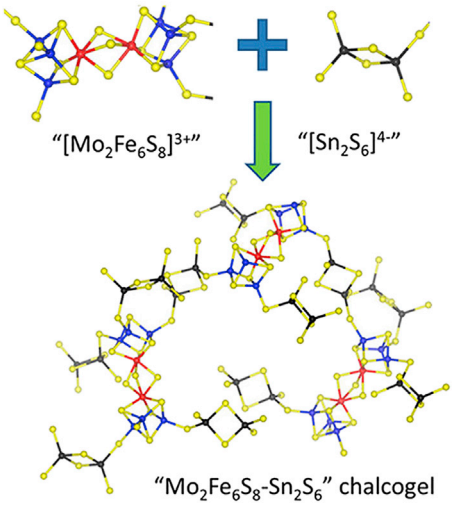


**Figure 8. Illustration of the $Mo_2Fe_6S_8$-$Sn_2S_6$ Biomimetic Chalcogel Building Block Self-Assembly Scheme**
Reproduced from Banerjee et al.,[31] with permission. Copyright 2015, American Chemical Society.

sulfide chalcogels,[31] (ii) layered mixed-valence double-hydroxide nanosheets,[56] (iii) plasmonic gold-metal oxide nanocomposites,[55,89] (iv) semiconductor-nitrogenase biohybrids,[26] and (v) plasmonic gold-black silicon nanostructures.[57]

In chronological order, each of these cases is described below. It must be noted that while the processes in this section use $N_2$ and $H_2O$ feedstocks, generating them will require the use of renewable energy. If the process produces a mix of products, such as $H_2$, $N_2$, and $O_2$, the need to separate them from the $NH_3$ will require additional energy.

In the chalcogels, double-cubane $[Mo_2Fe_6S_8]^{3+}$ cluster units, interconnected through $[Sn_2S_6]^{4-}$ ligands, create an amorphous network, considered a solid-state analog of the nitrogen-reducing nitrogenase enzymes (Figure 8).[31] The high density of strong visible-light-absorbing, linked molybdenum-iron sulfur clusters enhance the probability of light-induced, aqueous-phase, multi-electron $N_2$ reduction processes responsible for the formation of $NH_3$ under ambient conditions.

Mixed-valence $[M_{1-x}^{2+}M_x^{3+}(OH)_2]^{q+}(A_n^-)_{q/n}\cdot yH_2O$ layered double-hydroxide (LDH) nanosheets, where $M^{2+}$ = Zn, Ni, Cu and $M^{3+}$ = Al, Cr, exhibit intense UV and visible light absorption and display high photoreactivity for the reduction of $N_2$ to $NH_3$ under aqueous-phase ambient conditions (Figure 9).[56] The CuCr-LDH nanosheets in particular show high reactivity with 500-nm monochromatic light, the origin of which stems from oxygen vacancies, distortion of the nanosheets, and compressive strain. Acting synergistically, these effects boost the chemisorption and activation of $N_2$ and $H_2O$, intensify the harvesting of visible light, and thereby enhance the rate of formation of $NH_3$.

Gold nanocrystals on the surface of a niobium-doped strontium titanate film, coated with a nanometer zirconium-zirconium oxide layer, when exposed to visible light, selectively converted $N_2$-saturated $H_2O$ to $NH_3$ on the $ZrO_x$@Zr and $O_2$ on the Au@Nb:$SrTiO_3$ (Figure 10).[55] Visible-light plasmonic excitation of the Au nanocrystals (e.g., interband and/or intraband, near-field, hot electron effects) enables charge separation at the Au@Nb-$SrTiO_3$ interface. The photogenerated holes cause oxidation of $H_2O$ to $O_2$ at the Au@Nb-$SrTiO_3$ surface while the photogenerated electrons injected into the conduction band of $SrTiO_3$ reduce the $N_2$ at the $ZrO_x$@Zr surface.

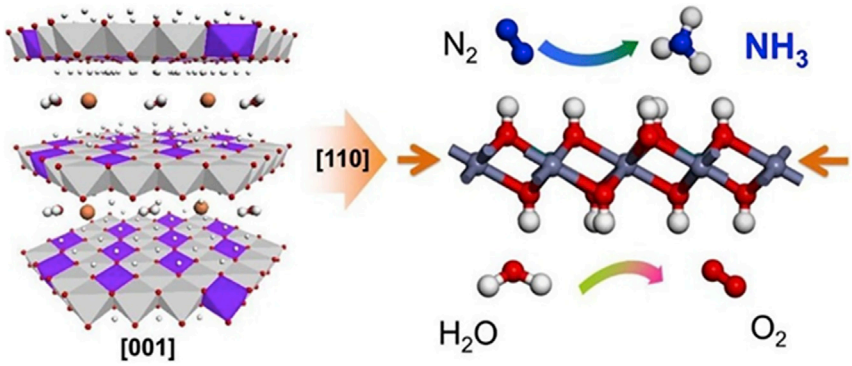


**Figure 9. (Left) Illustration of the Structure of the LDH Nanosheets with Defective $MO_6$ Octahedral Building Blocks at the Edge or Surface and (Right) Schematic of the Nitrogen Fixation Chemistry on the LDH Nanosheet**

Reproduced from Zhao et al.,[56] with permission. Copyright 2017, Wiley-VCH Verlag GmbH & Co. KGaA.

In a related recent study, surface oxygen vacancies of plasmon-enhanced rutile $TiO_2$/Au nanorods were tuned by atomic layer deposition.[89] The resulting deposited surface oxygen vacancies in the outer amorphous $TiO_2$ (a-$TiO_2$) thin layer not only promoted absorption and activation of $N_2$ but also facilitated $N_2$ reduction to $NH_3$ by the excited electrons from $TiO_2$ and Au surface plasmons. The photocatalytic $N_2$ reduction was investigated by immersing the photoelectrodes into $N_2$-saturated water with continuous $N_2$ bubbling under irradiation. As a result, the $NH_3$ production rate increased from 5.1 nmol $cm^{-2}$ $h^{-1}$ over bare $TiO_2$ to 13.4 nmol $cm^{-2}$ $h^{-1}$ over $TiO_2$/Au/a-$TiO_2$.

Inspired by the mild conditions of biological nitrogen fixation enabled by the enzyme nitrogenase, powered in nature by the chemical energy of adenosine 5′-triphosphate (ATP) hydrolysis, it has been found that photosensitization of nitrogenase molybdenum-iron protein by cadmium sulfide nanocrystals is able to drive the enzymatic reduction of $N_2$ to $NH_3$ (Figure 11).[26] The light harvesting in the CdS-MoFe nitrogenase bio-mimic replaces the driving force of ATP hydrolysis in the ATP-nitrogenase enzyme and reduces $N_2$ at a turnover frequency that is 63% of the nitrogenase complex operating under optimal conditions. This work is an elegant demonstration of the potential of "designer" semiconductor-nitrogenase bio-nanocomposites for the solar-powered generation of $NH_3$.

Solar ammonia and solar ammonium sulfate fertilizer can be produced by the photocatalytic reduction of $N_2$ by $H_2O$ using a plasmonic gold nanocrystal black silicon light absorber co-assembly (Figure 12).[57] Black silicon comprises a vertical Si nanorod assembly grown on a p-doped Si wafer, obtained by etching in aqueous HF. It appears visually black by suppressing optical reflection through enhanced multiple scattering and broadband optical absorption of light incident on the nano-structure. The active photocatalyst is prepared by growing gold nanocrystals on the Si nanorods and a film of Cr on the back side of the Si wafer. This multilayer structure essentially functions as a wireless photoelectrochemical cell able to perform redox reactions at different areas of the cell.

In brief, when light impinges on the Au@Si@Cr nanostructure immersed in $H_2O$, photogenerated electrons transported from Si to Au reduce the $N_2$ and $H_2O$ to $NH_3$ at the Au@Si interface. Gold plasmonic effects in Au@Si@Cr enhance this

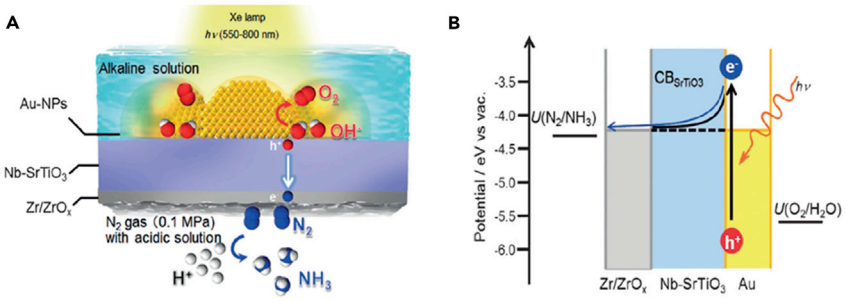


**Figure 10. Photocatalytic Nitrogen Reduction to Ammonia at Plasmonic Gold-Metal Oxide Nanocomposite**

(A) Schematic of the $NH_3$ synthesis device comprising the Nb-SrTiO3 photoelectrode loaded with Au-NPs and a $Zr/ZrO_x$ thin film.

(B) Energy-level diagram of the plasmon-induced $NH_3$ synthesis device.

Reproduced from Oshikiri et al.,[55] with permission. Copyright 2016, Wiley-VCH Verlag GmbH & Co. KGaA.

reduction process compared with Si@Cr devoid of Au. Concurrently, photogenerated holes transported from the Si to Cr oxidize the $H_2O$ to $O_2$ at the Cr film. In the presence of aqueous sulfite $SO_3^{2-}$, the holes oxidize $SO_3^{2-}$ to sulfate $SO_4^{2-}$ at the Cr film, according to the redox reaction equation $N_2 + 3H_2SO_3 + 3H_2O \rightarrow 2H_2SO_4 + (NH_4)_2SO_4$.

## Fact or Artifact

The nitrogen reduction reaction to ammonia in aqueous media driven electrochemically, photoelectrochemically, or photochemically is an extremely demanding reaction. The low solubility of $N_2$ in water coupled with currently achieved low conversions and conversion rates to $NH_3$ means claims of proof-of-product could turn out to be false positives. Artifacts of this type can originate from nitrogen impurities in the $^{14}N_2$ feed gas as well as $^{15}N$ isotopically labeled impurities in $^{15}N_2$ feed gas used to substantiate the $2N_2 + 3H_2O \rightarrow 2NH_3 + 3/2O_2$ reduction reaction. It is recommended that conversions, no matter how low, be reported, the purity of the $^{14}N_2$ and $^{15}N_2$ feed gases be at least 99.999%, and the type and amount of impurities, even at these low levels, be identified.

## Energy-Efficiency Analysis

Overall, there are a number of different routes and strategies for ammonia production using solar energy as summarized in Figure 2. In this section, we present a high-level analysis of the energy requirements of the strategies discussed in this paper. The goal is to highlight the advantages and disadvantages of the various strategies and identify opportunities for future research. The major assumptions used in this analysis are listed in Table 1, while a summary of the results is illustrated in Figure 13. We study six strategies, labeled A through F, where the results for each strategy are shown in the corresponding panels of Figure 13.

In terms of primary energy input, the conventional ammonia process consumes 30.5 MJ/kg-$NH_3$ (Figure 13A) in the form of fossil energy (natural gas), with steam reforming for hydrogen production being the major energy driver, accounting for approximately 75% of the total energy input. The remaining energy consumption (25.2%) comes, primarily, from gas compression, for the ammonia synthesis step, and refrigeration for ammonia separation. There are three interesting observations. First, in addition to accounting for the majority of the energy input, the use of methane for hydrogen production also leads to a $CO_2$-emitting stream, which is not, in general, the case in other fossil-fuel-based chemical production systems.

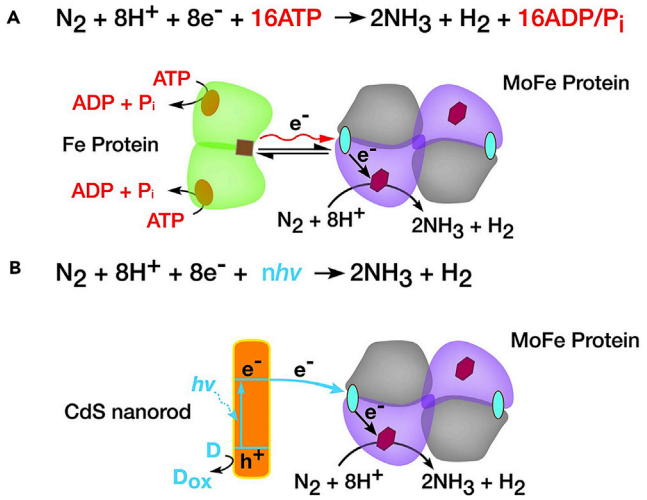


**Figure 11. Reaction Schemes for $N_2$ Reduction at Semiconductor-Nitrogenase Biohybrids**

(A and B) Schematic of reaction schemes for $N_2$ reduction to $NH_3$ by (A) nitrogenase and (B) the CdS:MoFe protein bio-hybrids. Reproduced from Brown et al.,[26] with permission. Copyright 2016, American Association for the Advancement of Science.

Second, the recovery of nitrogen from air is essentially replaced with the removal of $CO_2$ from a stream containing $H_2$, $N_2$, and $CO_2$. The implication of this replacement is that a power requirement, for a cryogenic air separation plant, has been replaced by a heating requirement, for the $CO_2$-amine separation, which can be met internally through heat integration (note the red arrow from the steam reforming to the CO & $CO_2$ removal block in Figure 13A). Third, if we use solar heat and electricity to energize this process, for consistency with the renewable strategies discussed next, there remains a 16.4 MJ/kg-$NH_3$ energy requirement met using natural gas, thereby leading to $CO_2$ emissions which, however, can be reduced if ammonia and urea plants are integrated.[94]

Conceptually, the simplest approach to avoid $CO_2$ emissions is by producing hydrogen from water electrolysis, rather than methane, using solar electricity. The simplest source of nitrogen will be air separation. The renewable hydrogen production and air separation blocks can then be combined, in principle, with either a traditional Haber-Bosch reactor system employing renewable electricity for compression (Figure 13B) or a renewable ammonia synthesis block—for instance, a molybdenum-based redox cycle[58] (Figure 13C). Given the low solar-to-power conversion efficiency, the overall primary energy input increases: for the hydrogen production block, from 16.4 MJ/kg-$NH_3$ of methane to 236.7 MJ/kg-$NH_3$ of solar energy. Low energy efficiency leads, in general, to high production cost because the unit capital cost ($/kg-$NH_3$) for solar energy harvesting increases, but from an environmental standpoint the two strategies address the major impact of the Haber-Bosch process, namely, the emission of $CO_2$ by utilizing solar energy instead of natural gas.

The ammonia synthesis block of the two strategies based on water electrolysis (B and C) consumes $H_2$ and $N_2$, which means that two preparatory blocks are necessary for hydrogen (electrolysis) and nitrogen (air separation) production. A conceptual simplification can be achieved if ammonia is produced from water and nitrogen through, for example, electrocatalysis (Figure 13D). The advantage of this strategy, compared with strategies B and C, is that it employs two instead of three major blocks, and if a high faradaic efficiency (e.g., 50%) is achieved, then the overall solar

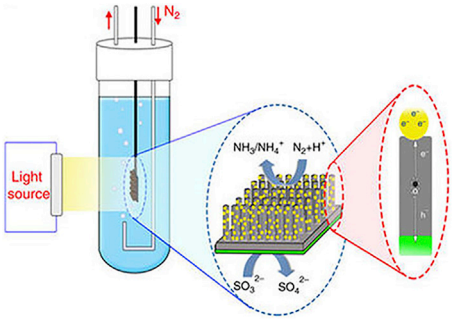


**Figure 12. Photocatalytic Nitrogen Reduction over Plasmonic Gold-Black Silicon Nanostructure**
Illustration of (left) the plasmonic enhanced gold nanocrystal black silicon chromium light absorber mounted in the photoreactor filled with $H_2O$ and purged with $N_2$, (middle) $N_2$ reduction and $SO_3^{2-}$ oxidation reactions occurring at the Au and Cr, and (right) photogeneration and transport of electrons and holes to the Au and Cr, respectively. Reproduced from Ali et al.,[57] with permission. Copyright 2016, Macmillan Publishers Limited, part of Springer Nature.

energy consumption decreases to 190.5 MJ/kg-$NH_3$. A disadvantage of this strategy is that electrocatalytic technologies for the conversion of $H_2O$ and $N_2$ to ammonia are in their infancy, especially when compared with water electrolysis.

Strategies B, C, and D employ solar energy, rather than natural gas, but do so through solar electricity production. In the best case (strategy D), 27.2 MJ of solar electricity displace 16.4 MJ of natural gas, which would be required to manufacture the same amount of ammonia (1 kg). However, the production of 27.2 MJ of electricity requires 89 MJ of natural gas, assuming a 40% natural-gas-to-electricity conversion efficiency. In other words, if solar electricity is available, its use for ammonia production is suboptimal, at least until the electricity mix becomes nearly 100% renewable.

The replacement of the electrocatalytic conversion with a photocatalytic one (Figure 13E), has the advantage that it does not require electricity. If the solar-to-chemical conversion (SCC) efficiency of the photocatalytic block is 10%, the solar energy consumption is 208.3 MJ/kg-$NH_3$. While this number is higher than the solar input in strategy D, the advantage of strategy E is that it can be potentially cheaper because it does not employ a (likely expensive) electrocatalytic step.

Conceptually, strategy F represents a major departure from all previous strategies in that it employs $CH_4$ as a reducing agent via an aluminum-based redox cycle[95] (Figure 13F), which has similar net solar energy input (171.8 MJ/kg-$NH_3$) for the ammonia synthesis similar to that of strategies D and E, assuming a 25% solar-to-fuel efficiency for the redox block, which has two significant advantages. First, it reduces the solar energy input for ammonia synthesis to 115.8 from 208.3 MJ/kg-$NH_3$, assuming a 45% solar-to-heat efficiency for the redox block, which represents a 40% advantage over strategy D. However, strategy F co-produces syngas (which can be further converted to, for example, methanol), with, most importantly, an efficiency comparable with traditional methane reforming. Thus, strategy F can be viewed as a two-purpose strategy: (1) it produces syngas from methane with an 86% efficiency; and (2) produces ammonia with a competitive solar requirement.

## Toward the Solar Ammonia Refinery

The yields of solar ammonia by all of the above light-powered $N_2$ reduction systems are currently in the nmol $g_{cat}^{-1}$ $h^{-1}$ to μmol $g_{cat}^{-1}$ $h^{-1}$ range and insufficient

**Table 1. Assumptions for Energy Analysis**

| | |
|---|---|
| Fossil-to-power efficiency | 0.37[90] |
| Fossil-to-heat efficiency | 0.86[90] |
| Solar-to-power efficiency | 0.15[91,92] |
| Solar-to-heat efficiency | 0.45[91,92] |
| $N_2$ to $NH_3$ conversion in all strategies | 90 mol% |
| Solar-to-chemical energy conversion efficiency (SCC) for photocatalytic conversion | 10% |
| Faradaic efficiency (FE) for electrocatalytic conversion | 50% |
| Air separation energy consumption | 0.421 kWh/kg-$N_2$[93] |
| Energy consumption for electrolytic $H_2$ production | 50 kWh/kg-$H_2$[34] |

The data for the conventional ammonia process are taken from the Aspen Plus (V8.6) Ammonia Model. The energy content of $O_2$, after air separation, is neglected.

for industrial applications. Nevertheless, many opportunities exist to optimize the light harvesting, conversion rate, energy efficiency, and economic viability of the process. This can be accomplished through creative materials chemistry, purposeful reactor engineering, and designed computer intelligence of the activity of (photo)catalysts and performance of (photo)reactors. The vision to replace the fossil-powered Haber-Bosch ammonia process by a green ammonia process, ultimately to one using just $N_2$, $H_2O$, and sunlight, and operating under ambient conditions of temperature and pressure, remains an exciting challenge for future research. The realization of this vision can be a driving force toward a carbon-free future.

If it proves possible to produce solar ammonia from just $N_2$, $H_2O$, and sunlight on an industrially significant scale, efficiency, and cost, then three atoms of hydrogen and one atom of nitrogen, which once changed the world, may in the future help save the world!

## Postscript

In percolating over the vision of a solar ammonia refinery in a renewable energy world bent on decarbonization of fossil-powered systems, a challenge is how to make a credible case for an electricity-to-chemical energy technology. An emerging school of thought is that storing electrical energy as chemical energy is not, in general, a good proposition, unless it is electricity that otherwise would be wasted. In Germany, where renewable energy plays a major role in the economy, one can imagine a scenario when the sun does shine and the wind does blow whereby there may be more electricity than could ever be consumed, so it has to be stored.

So the question becomes how best to store excess electricity. One obvious answer is to store it using batteries with about 80% efficiency round-trip for conversion back to electricity. Another is to charge electric vehicles with a 70% efficiency for electricity to electric motor. Both of these energy-storage alternatives are experiencing rapid development and deployment, and currently surpass electricity-to-chemical energy in the form of a fuel used to power a 30% efficient internal combustion engine.

In the short term, battery and electric vehicle storage are competing technologies with which renewable electricity-to-chemical energy technologies must compete. Longer term, in a fully electrified world, storage of renewable energy in base

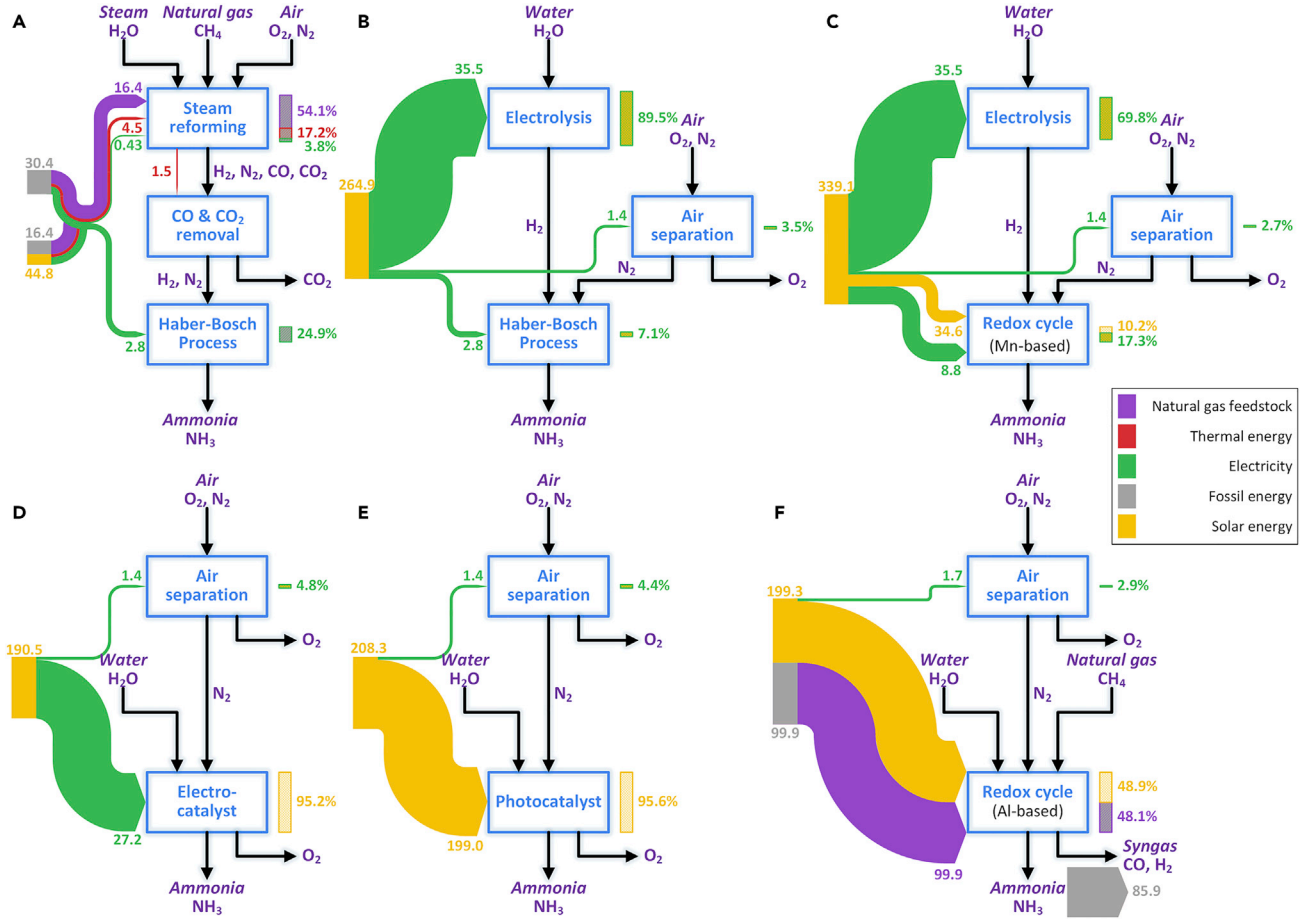


**Figure 13. Results of Energy-Efficiency Analysis for Ammonia Production Strategies**

(A) Conventional Haber-Bosch strategy.

(B) Renewable hydrogen production and air separation combined with traditional Haber-Bosch reactor system.

(C) Renewable hydrogen production and air separation combined with a molybdenum-based redox cycle.

(D) Electrocatalytic strategy.

(E) Photocatalytic strategy.

(F) Aluminum-based redox cycle using $CH_4$ as a reducing agent.

The width of each stream on the left of each block and the numbers represent energy flow (MJ/kg-$NH_3$). The height of each column on the right of each block represents the share of total energy input.

chemicals, which include petroleum, inorganic, polymer, pharmaceutical, consumer, and specialty products, will grow in importance. Today, the production of base chemicals is energy, greenhouse gas, and capital intensive, and it is projected that annual global sales will expand from $3.5 trillion in 2017 to $6.3 trillion in 2030. To this end, the development of electricity-to-chemical technologies with a competitive energy efficiency and economic advantage makes sense.

Another school of thought aims to capture the "solar advantage," namely to convert solar energy directly into chemical energy through photochemistry, photothermal chemistry, and solar thermal chemistry, thereby avoiding electricity altogether. Realization of the vision of a solar-to-chemicals (S2C) industry will require long-term research and development designed to achieve materials, reactor, and process engineering performance metrics and meet energy-efficiency, economic, and carbon-footprint targets.

## ACKNOWLEDGMENTS

G.A.O. is a Government of Canada Research Chair in Materials Chemistry and Nanochemistry. Financial support for the work of the solar fuels team was provided by the Ontario Ministry of Research Innovation, Ministry of Economic Development, Employment and Infrastructure, Ministry of the Environment and Climate Change (MOECC), Best in Science (MOECC), Connaught Innovation Fund, Connaught Global Challenge, Solutions 2030 Challenge Fund Ontario Center of Excellence, Low Carbon Innovation Fund Ministry of Research, Innovation and Science, Imperial Oil, and the Natural Sciences and Engineering Research Council of Canada. Critical reading and insightful feedback of the article by Aldo Steinfeld (Swiss Federal Institute of Technology Zurich), Tierui Zhang (Technical Institute of Physics and Chemistry, Chinese Academy of Science), Michael Bender (BASF), Erik Haites (Margaree Consultants, Toronto), and Robert Morris (University of Toronto), is deeply appreciated. The proof-reading of this article by Bob Davies proved to be invaluable.

## REFERENCES

1. van der Ham, C.J.M., Koper, M.T.M., and Hetterscheid, D.G.H. (2014). Challenges in reduction of dinitrogen by proton and electron transfer. Chem. Soc. Rev. *43*, 5183–5191.
2. Chirik, P.J. (2009). One electron at a time. Nat. Chem. *1*, 520–522.
3. Ertl, G. (2008). Reactions at surfaces: from atoms to complexity (Nobel lecture). Angew. Chem. Int. Ed. *47*, 3524–3535.
4. Honkala, K., Hellman, A., Remediakis, I.N., Logadottir, A., Carlsson, A., Dahl, S., Christensen, C.H., and Norskov, J.K. (2005). Ammonia synthesis from first-principles calculations. Science *307*, 555–558.
5. Michalsky, R., Pfromm, P.H., and Steinfeld, A. (2015). Rational design of metal nitride redox materials for solar-driven ammonia synthesis. Interface Focus *5*, 20140084.
6. Service, R.F. (2014). Chemistry. New recipe produces ammonia from air, water, and sunlight. Science *345*, 610.
7. Rosca, V., Duca, M., de Groot, M.T., and Koper, M.T.M. (2009). Nitrogen cycle electrocatalysis. Chem. Rev. *109*, 2209–2244.
8. Coric, I., Mercado, B.Q., Bill, E., Vinyard, D.J., and Holland, P.L. (2015). Binding of dinitrogen to an iron-sulfur-carbon site. Nature *526*, 96–99.
9. Howarth, R.W. (2008). Coastal nitrogen pollution: a review of sources and trends globally and regionally. Harmful Algae *8*, 14–20.
10. Pickett, C.J., and Talarmin, J. (1985). Electrosynthesis of ammonia. Nature *317*, 652–653.
11. Christensen, C.H., Johannessen, T., Sorensen, R.Z., and Norskov, J.K. (2006). Towards an ammonia-mediated hydrogen economy? Catal. Today *111*, 140–144.
12. van Kessel, M.A., Speth, D.R., Albertsen, M., Nielsen, P.H., Op den Camp, H.J., Kartal, B., Jetten, M.S.M., and Lucker, S. (2015). Complete nitrification by a single microorganism. Nature *528*, 555.
13. Yandulov, D.V., and Schrock, R.R. (2003). Catalytic reduction of dinitrogen to ammonia at a single molybdenum center. Science *301*, 76–78.
14. U.S. Geological Survey (2016). Mineral Commodity Summaries 2016: U.S. Geological Survey (Washington, DC, USA: U.S. Government Publishing Office), p. 118.
15. Schnitkey, G. (2017). Fertilizer costs in 2017 and 2018. Farmdoc Daily *7*, 3.
16. Kaag, C.S., and Krishnamurthy, V.N. (2010). The fertilizer encyclopedia. Ref. User Serv. Q. *50*, 82–83.
17. Stewart, W.M., Dibb, D.W., Johnston, A.E., and Smyth, T.J. (2005). The contribution of commercial fertilizer nutrients to food production. Agron J. *97*, 1–6.
18. International Fertilizer Industry Association (2009). Fertilizers, Climate Change and Enhancing Agricultural Productivity Sustainably (Paris, France: IFA).
19. Vaclav, S. (2004). Enriching the Earth (The MIT Press).
20. Li, S.J., Bao, D., Shi, M.M., Wulan, B.R., Yan, J.M., and Jiang, Q. (2017). Amorphizing of Au nanoparticles by $CeO_x$-RGO hybrid support towards highly efficient electrocatalyst for $N_2$ reduction under ambient conditions. Adv. Mater. *29*, 1700001.
21. Shi, M.M., Bao, D., Wulan, B.R., Li, Y.H., Zhang, Y.F., Yan, J.M., and Jiang, Q. (2017). Au sub-nanoclusters on TiO2 toward highly efficient and selective electrocatalyst for $N_2$ conversion to $NH_3$ at ambient conditions. Adv. Mater. *29*, 1606550.
22. Jackson, R.B., Canadell, J.G., Le Quere, C., Andrew, R.M., Korsbakken, J.I., Peters, G.P., and Nakicenovic, N. (2016). Reaching peak emissions. Nat. Clim. Chang. *6*, 7.
23. Kitano, M., Kanbara, S., Inoue, Y., Kuganathan, N., Sushko, P.V., Yokoyama, T., Hara, M., and Hosono, H. (2015). Electride support boosts nitrogen dissociation over ruthenium catalyst and shifts the bottleneck in ammonia synthesis. Nat. Commun. *6*, 6731.
24. Ritter, S.K. (2008). Iron's star rising. Chem. Eng. News *86*, 53–57.
25. Ceresana (2012). Market Study: Ammonia (UC-3705).https://www.ceresana.com/upload/Marktstudien/brochueren/Ceresana_-_Brochure_Market_Study_Ammonia.pdf.
26. Brown, K.A., Harris, D.F., Wilker, M.B., Rasmussen, A., Khadka, N., Hamby, H., Keable, S., Dukovic, G., Peters, J.W., Seefeldt, L.C., and King, P.W. (2016). Light-driven dinitrogen reduction catalyzed by a CdS:nitrogenase MoFe protein biohybrid. Science *352*, 448–450.
27. Lu, Y.H., Yang, Y., Zhang, T.F., Ge, Z., Chang, H.C., Xiao, P.S., Xie, Y.Y., Hua, L., Li, Q.Y., Li, H.Y., et al. (2016). Photoprompted hot electrons from bulk cross-linked graphene materials and their efficient catalysis for atmospheric ammonia synthesis. ACS Nano *10*, 10507–10515.
28. Appl, M. (1994). The development of the ammonia technology. Chem. Tech. *46*, 125–135.
29. Fuerst, T., Lundin, S., Zhang, Z., Liguori, S., Way, D., and Wolden, C. (2017). Dense metallic membrane reactor synthesis of ammonia at moderate conditions and low cost Paper presented at the $NH_3$ Fuel Conference.
30. Twygg, M.V. (1989). Catalyst Handbook, 2nd Edition (Oxford University Press).
31. Banerjee, A., Yuhas, B.D., Margulies, E.A., Zhang, Y.B., Shim, Y., Wasielewski, M.R., and Kanatzidis, M.G. (2015). Photochemical nitrogen conversion to ammonia in ambient conditions with FeMoS-chalcogels. J. Am. Chem. Soc. *137*, 2030–2034.
32. Bao, D., Zhang, Q., Meng, F.L., Zhong, H.X., Shi, M.M., Zhang, Y., Yan, J.M., Jiang, Q., and Zhang, X.B. (2017). Electrochemical reduction of $N_2$ under ambient conditions for artificial $N_2$ fixation and renewable energy storage using $N_2/NH_3$ cycle. Adv. Mater. *29*, 1604799.
33. Koleli, F., and Kayan, D.B. (2010). Low overpotential reduction of dinitrogen to ammonia in aqueous media. J. Electroanal. Chem. *638*, 119–122.

34. U.S. Department of Energy (2015). DOE Technical Targets for Hydrogen Production from Electrolysis. Energy.gov. Available at: https://energy.gov/eere/fuelcells/doe-technical-targets-hydrogen-production-electrolysis. Accessed February 12, 2018.

35. LAZARD (2017). Lazard's Levelized Cost of Energy Analysis—Version 11.0.https://www.lazard.com/media/450337/lazard-levelized-cost-of-energy-version-110.pdf.

36. Chen, S.M., Perathoner, S., Ampelli, C., Mebrahtu, C., Su, D.S., and Centi, G. (2017). Electrocatalytic synthesis of ammonia at room temperature and atmospheric pressure from water and nitrogen on a carbon-nanotube-based electrocatalyst. Angew. Chem. Int. Ed. *56*, 2699–2703.

37. Golabiewska, A., Malankowska, A., Jarek, M., Lisowski, W., Nowaczyk, G., Jurga, S., and Zaleska-Medynska, A. (2016). The effect of gold shape and size on the properties and visible light-induced photoactivity of Au-$TiO_2$. Appl. Catal. B Environ. *196*, 27–40.

38. Michalsky, R., and Steinfeld, A. (2017). Computational screening of perovskite redox materials for solar thermochemical ammonia synthesis from $N_2$ and $H_2O$. Catal. Today *286*, 124–130.

39. Kyriakou, V., Garagounis, I., Vasileiou, E., Vourros, A., and Stoukides, M. (2017). Progress in the electrochemical synthesis of ammonia. Catal. Today *286*, 2–13.

40. Chen, G.F., Cao, X.R., Wu, S.Q., Zeng, X.Y., Ding, L.X., Zhu, M., and Wang, H.H. (2017). Ammonia electrosynthesis with high selectivity under ambient conditions via a $Li^+$ incorporation strategy. J. Am. Chem. Soc. *139*, 9771–9774.

41. Murakami, T., Nishikiori, T., Nohira, T., and Ito, Y. (2003). Electrolytic synthesis of ammonia in molten salts under atmospheric pressure. J. Am. Chem. Soc. *125*, 334–335.

42. Murakami, T., Nishikiori, T., Nohira, T., and Ito, Y. (2005). Investigation of anodic reaction of electrolytic ammonia synthesis in molten salts under atmospheric pressure. J. Electrochem. Soc. *152*, D75–D78.

43. Murakami, T., Nohira, T., Goto, T., Ogata, Y.H., and Ito, Y. (2005). Electrolytic ammonia synthesis from water and nitrogen gas in molten salt under atmospheric pressure. Electrochim. Acta *50*, 5423–5426.

44. Shipman, M.A., and Symes, M.D. (2017). A re-evaluation of Sn(II) phthalocyanine as a catalyst for the electrosynthesis of ammonia. Electrochim. Acta *258*, 618–622.

45. Singh, A.R., Rohr, B.A., Schwalbe, J.A., Cargnello, M., Chan, K., Jaramillo, T.F., Chorkendorff, I., and Norskov, J.K. (2017). Electrochemical ammonia synthesis-the selectivity challenge. ACS Catal. *7*, 706–709.

46. Shipman, M.A., and Symes, M.D. (2017). Recent progress towards the electrosynthesis of ammonia from sustainable resources. Catal. Today *286*, 57–68.

47. Liu, C., Sakimoto, K.K., Colon, B.C., Silver, P.A., and Nocera, D.G. (2017). Ambient nitrogen reduction cycle using a hybrid inorganic-biological system. Proc. Natl. Acad. Sci. USA *114*, 6450–6455.

48. Shanmugam, K.T., and Valentine, R.C. (1975). Microbial production of ammonium ion from nitrogen. Proc. Natl. Acad. Sci. USA *72*, 136–139.

49. Kitano, M., Inoue, Y., Yamazaki, Y., Hayashi, F., Kanbara, S., Matsuishi, S., Yokoyama, T., Kim, S.W., Hara, M., and Hosono, H. (2012). Ammonia synthesis using a stable electride as an electron donor and reversible hydrogen store. Nat. Chem. *4*, 934–940.

50. Kitano, M., Inoue, Y., Sasase, M., Kishida, K., Kobayashi, Y., Nishiyama, K., Tada, T., Kawamura, S., Yokoyama, T., Hara, M., and Hosono, H. (2018). Self-organized ruthenium-barium core-shell nanoparticles on a mesoporous calcium amide matrix for efficient low-temperature ammonia synthesis. Angew. Chem. Int. Ed. *57*, 2648–2652.

51. Gong, Y., Wu, J., Kitano, M., Wang, J., Ye, T.N., Li, J., Kobayashi, Y., Kishida, K., Abe, H., Niwa, Y., et al. (2018). Ternary intermetallic LaCoSi as a catalyst for $N_2$ activation. Nat. Catal. *1*, 178–185.

52. Peng, P., Li, Y., Cheng, Y.L., Deng, S.B., Chen, P., and Ruan, R. (2016). Atmospheric pressure ammonia synthesis using non-thermal plasma assisted catalysis. Plasma Chem. Plasma Process. *36*, 1201–1210.

53. Hong, J.M., Aramesh, M., Shimoni, O., Seo, D.H., Yick, S., Greig, A., Charles, C., Prawer, S., and Murphy, A.B. (2016). Plasma catalytic synthesis of ammonia using functionalized-carbon coatings in an atmospheric-pressure non-equilibrium discharge. Plasma Chem. Plasma Process. *36*, 917–940.

54. Zhu, D., Zhang, L.H., Ruther, R.E., and Hamers, R.J. (2013). Photo-illuminated diamond as a solid-state source of solvated electrons in water for nitrogen reduction. Nat. Mater. *12*, 836–841.

55. Oshikiri, T., Ueno, K., and Misawa, H. (2016). Selective dinitrogen conversion to ammonia using water and visible light through plasmon-induced charge separation. Angew. Chem. Int. Ed. *55*, 3942–3946.

56. Zhao, Y.F., Zhao, Y.X., Waterhouse, G.I.N., Zheng, L.R., Cao, X.Z., Teng, F., Wu, L.Z., Tung, C.H., O'Hare, D., and Zhang, T.R. (2017). Layered-double-hydroxide nanosheets as efficient visible-light-driven photocatalysts for dinitrogen fixation. Adv. Mater. *29*, 1703828.

57. Ali, M., Zhou, F.L., Chen, K., Kotzur, C., Xiao, C.L., Bourgeois, L., Zhang, X.Y., and MacFarlane, D.R. (2016). Nanostructured photoelectrochemical solar cell for nitrogen reduction using plasmon-enhanced black silicon. Nat. Commun. *7*, 11335.

58. Michalsky, R., Parman, B.J., Amanor-Boadu, V., and Pfromm, P.H. (2012). Solar thermochemical production of ammonia from water, air and sunlight: thermodynamic and economic analyses. Energy *42*, 251–260.

59. S.P.F. LLC (2017). C-Free Renew. Retrieved from solarhydrogensystem.com [Accessed January 7, 2018].

60. Yara (2017). Solar ammonia. Retrieved from yara.com [Accessed January 7, 2018].

61. Sable Chemical Industries (2018). Retrieved from http://www.sablechemicals.com/technology [Accessed March 9, 2018].

62. Brown, T. (2018). Renewable ammonia demonstration plant announced in South Australia. Ammonia Industry. Retrieved from: https://ammoniaindustry.com/renewable-ammonia-demonstration-plant-announced-in-south-australia/ [Accessed March 6, 2018].

63. Furuya, N., and Yoshiba, H. (1990). Electroreduction of nitrogen to ammonia on gas-diffusion electrodes loaded with inorganic catalyst. J. Electroanal. Chem. *291*, 269–272.

64. Marnellos, G., and Stoukides, M. (1998). Ammonia synthesis at atmospheric pressure. Science *282*, 98–100.

65. Licht, S., Cui, B.C., Wang, B.H., Li, F.F., Lau, J., and Liu, S.Z. (2014). AMMONIA SYNTHESIS ammonia synthesis by $N_2$ and steam electrolysis in molten hydroxide suspensions of nanoscale $Fe_2O_3$. Science *345*, 637–640.

66. Wang, W.B., Cao, X.B., Gao, W.J., Zhang, F., Wang, H.T., and Ma, G.L. (2010). Ammonia synthesis at atmospheric pressure using a reactor with thin solid electrolyte $BaCe_{0.85}Y_{0.15}O_3$-alpha membrane. J. Memb. Sci. *360*, 397–403.

67. Amar, I.A., Lan, R., Petit, C.T.G., and Tao, S.W. (2011). Solid-state electrochemical synthesis of ammonia: a review. J. Solid State Electr. *15*, 1845–1860.

68. Amar, I.A., Petit, C.T.G., Zhang, L., Lan, R., Skabara, P.J., and Tao, S. (2011). Electrochemical synthesis of ammonia based on doped-ceria-carbonate composite electrolyte and perovskite cathode. Solid State Ion. *201*, 94–100.

69. Hydrofuel Inc. (2016). New evidence on greener energy solutions to be presented at Los Angeles conference. Retrieved from www.nh3fuel.com [Accessed January 7, 2018].

70. Hydrofuel Inc. (2006). Back to the future. Retrieved from www.nh3fuel.com [Accessed January 7, 2018].

71. Hydrofuel Inc. (2015). UOIT MITACS research. Retrieved from nh3fuel.com/index.php?option=com_content&task=view&id=29&Itemid=36 [Accessed January 7, 2018].

72. Anderson, J.S., Rittle, J., and Peters, J.C. (2013). Catalytic conversion of nitrogen to ammonia by an iron model complex. Nature *501*, 84.

73. Kugler, K., Luhn, M., Schramm, J.A., Rahimi, K., and Wessling, M. (2015). Galvanic deposition of Rh and Ru on randomly structured Ti felts for the electrochemical $NH_3$ synthesis. Phys. Chem. Chem. Phys. *17*, 3768–3782.

74. Tsuneto, A., Kudo, A., and Sakata, T. (1994). Lithium-mediated electrochemical reduction of high-pressure $N_2$ to $NH_3$. J. Electroanal. Chem. *367*, 183–188.

75. Amar, I.A., Lan, R., and Tao, S.W. (2015). Synthesis of ammonia directly from wet nitrogen using a redox stable $La_{0.75}Sr_{0.25}Cr_{0.5}Fe_{0.5}O_3$-delta-$Ce_{0.8}Gd_{0.18}Ca_{0.02}O_2$-delta composite cathode. RSC Adv. *5*, 38977–38983.

76. Yun, D.S., Joo, J.H., Yu, J.H., Yoon, H.C., Kim, J.N., and Yoo, C.Y. (2015). Electrochemical ammonia synthesis from steam and nitrogen using proton conducting yttrium doped barium zirconate electrolyte with silver, platinum, and lanthanum strontium cobalt ferrite electrocatalyst. J. Power Sources *284*, 245–251.

77. Liu, Y.M., Su, Y., Quan, X., Fan, X.F., Chen, S., Yu, H.T., Zhao, H.M., Zhang, Y.B., and Zhao, J.J. (2018). Facile ammonia synthesis from electrocatalytic $N_2$ reduction under ambient conditions on N-doped porous carbon. ACS Catal. *8*, 1186–1191.

78. Hargreaves, J.S.J. (2014). Nitrides as ammonia synthesis catalysts and as potential nitrogen transfer reagents. Appl. Petrochem. Res. *4*, 3–10.

79. Alexander, A.M., Hargreaves, J.S.J., and Mitchell, C. (2012). The reduction of various nitrides under hydrogen: $Ni_3N$, $Cu_3N$, $Zn_3N_2$ and $Ta_3N_5$. Top. Catal. *55*, 1046–1053.

80. Yao, Y., Zhu, S., Wang, H., Li, H., and Shao, M. (2018). A spectroscopic study on the nitrogen electrochemical reduction reaction on gold and platinum surfaces. J. Am. Chem. Soc. *140*, 1496–1501.

81. Lan, R., Irvine, J.T., and Tao, S. (2013). Synthesis of ammonia directly from air and water at ambient temperature and pressure. Sci. Rep. *3*, 1145.

82. Lan, R., and Tao, S.W. (2013). Electrochemical synthesis of ammonia directly from air and water using a Li+/H+/NH4+ mixed conducting electrolyte. RSC Adv. *3*, 18016–18021.

83. Institute for Sustainable Process Technology (2017). Power to ammonia: from renewable energy to $CO_2$-free ammonia as chemical feedstock and fuel. Retrieved from http://www.ispt.eu/power-ammonia-renewable-energy-co2-free-ammonia-chemical-feedstock-fuel/ [Accessed January 7, 2018].

84. Siemens plc (2015). Green ammonia. Retrieved from http://www.siemens.co.uk/en/insights/potential-of-green-ammonia-as-fertiliser-and-electricity-storage.htm [Accessed January 7, 2018].

85. McEnaney, J.M., Singh, A.R., Schwalbe, J.A., Kibsgaard, J., Lin, J.C., Cargnello, M., Jaramillo, T.F., and Norskov, J.K. (2017). Ammonia synthesis from $N_2$ and $H_2O$ using a lithium cycling electrification strategy at atmospheric pressure. Energ. Environ. Sci. *10*, 1621–1630.

86. Peng, P., Cheng, Y., Hatzenbeller, R., Addy, M., Zhou, N., Schiappacasse, C., Chen, D., Zhang, Y., Anderson, E., Liu, Y., and Chen, P. (2017). Ru-based multifunctional mesoporous catalyst for low-pressure and non-thermal plasma synthesis of ammonia. International Journal of Hydrogen Energy, *42*, 19056–19066.

87. Schrauzer, G.N., and Guth, T.D. (1977). Photolysis of water and photoreduction of nitrogen on titanium-dioxide. J. Am. Chem. Soc. *99*, 7189–7193.

88. Li, X.M., Wang, W.Z., Jiang, D., Sun, S.M., Zhang, L., and Sun, X. (2016). Efficient solar-driven nitrogen fixation over carbon-tungstic-acid hybrids. Chem. Eur. J. *22*, 13819–13822.

89. Li, C., Wang, T., Zhao, Z.J., Yang, W., Li, J.F., Li, A., Yang, Z., Ozin, G.A., and Gong, J. (2018). Promoted fixation of molecular nitrogen with surface oxygen vacancies on plasmon-enhanced $TiO_2$ photoelectrodes. Angew. Chem. Int. Ed. https://doi.org/10.1002/anie.201713229.

90. Kim, J., Johnson, T.A., Miller, J.E., Stechel, E.B., and Maravelias, C.T. (2012). Fuel production from $CO_2$ using solar-thermal energy: system level analysis. Energ. Environ. Sci. *5*, 8417–8429.

91. Herron, J.A., Kim, J., Upadhye, A.A., Huber, G.W., and Maravelias, C.T. (2015). A general framework for the assessment of solar fuel technologies. Energ. Environ. Sci. *8*, 126–157.

92. Herron, J.A., and Maravelias, C.T. (2016). Assessment of solar-to-fuels strategies: photocatalysis and electrocatalytic reduction. Energy Technol. *4*, 1369–1391.

93. Aneke, M., and Wang, M.H. (2015). Potential for improving the energy efficiency of cryogenic air separation unit (ASU) using binary heat recovery cycles. Appl. Therm. Eng. *81*, 223–231.

94. Thambimuthu, K., Soltanieh, M., Abanades, J.C., Allam, R., Bolland, O., Davison, J., Feron, P., Goede, F., Herrera, A., Iijima, M. et al. (2005). Capture of $CO_2$. IPCC Special Report on Carbon Dioxide Capture Storage. 105–178.

95. Galvez, M.E., Halmann, M., and Steinfeld, A. (2007). Ammonia production via a two-step $Al_2O_3$/AlN thermochemical cycle. 1. Thermodynamic, environmental, and economic analyses. Ind. Eng. Chem. Res. *46*, 2042–2046.